Image Quality Assessment of In-House Phantom for Pediatric Computed Tomography

Audiena Gelung Prayitno,[1] Dafa Miftahuddin,[1] Aditya Prayugo Hariyanto,[1] M. Roslan A Gani,[2] and Endarko*[1]

[1]*Department of Physics, Faculty of Science and Analytical Data*
Institut Teknologi Sepuluh Nopember (ITS), Kampus ITS Sukolilo, Surabaya 60111
[2]*Department of Radiology, Dharmais Hospital National Cancer Center*
Jl. Letjen. S. Parman No.84-86, Jakarta Barat 11420

Abstract: Computed tomography (CT) offers several advantages. However, it involves a high dose of radiation exposure. In pediatric CT scans, reducing the radiation dose can lead to increased noise and lower image quality. Generally, there is a significant relationship between radiation dose and diagnostic image quality. This research investigates and analyzes the correlation between low-dose radiation and image quality in pediatric CT scans. This study used in house pediatric phantoms (7 year). Twelve artificial cylinder targets were fabricated with diameters 3, 5, 8, and 10 mm, and CT densities +100, -400, -750 HU. The image quality was performed using CT-Scan 128 slice with parameters of helical scanning using a low dose and standard dose and using 80 and 120 kV. For Signal noise to ratio (SNR), Contrast to Noise Ratio (CNR), Volumetric CT dose index (CTDIvol), SizeSpecific Dose Estimates (SSDE) also investigated. The effective value of the diameter for 7 years was 20.15 cm. Findings suggest, SSDE for in-house pediatric phantoms was found to be 3.71 mGy for low dose and 6.09 for standard dose. For image quality analysis, the low-dose CT protocol has a detection sensitivity of 100% for targets measuring $>$ 5mm in diameter.

Keywords: CT-Scan; Dose; Thorax;, Pediaitric

*Corresponding author: endarko@physics.its.ac.id

http://dx.doi.org/10.12962/j24604682.v21i2.20434
2460-4682

I. INTRODUCTION

CT scans deliver a higher dose of radiation than other X-ray diagnostic procedures. This concern is especially apparent in the pediatric population. This fact is because growing pediatric tissues are significantly more sensitive to ionizing radiation carcinogenesis than adults due to faster cell division, the probability of which increases with radiation dose. However, the dramatic increase in CT use is responsible for increasing medical exposure to ionizing radiation [1]. So, there is a need to ensure that radiation protection methods for CT procedures are optimized to keep dose levels to a minimum. Therefore, the potential risk of cancer due to radiation exposure is more significant in children. Although the sensitivity of pediatric radio is higher than that of adults, the number of pediatric CT examinations requested is increasing globally. In addition, children's longer lives give them more chances to live and increase awareness of malignancies from radiation exposure.

Significant effort has been focused on achieving the lowest possible radiation dose for pediatric patients, especially adjusting for size differences. Dose reduction is often associated with increased noise and artifacts affecting image interpretation [2]. The organ tissue type and the sensitivity of the scan indication should be considered during the adjustment of CT parameters. For example, it is acceptable to decrease the dose when a diagnosis is made of large lesions or during follow-up examinations. Reduction of mAs or kVp may also be justified in areas of relatively high contrast, such as lung parenchyma and bone, but may lead to poor diagnosis in the abdomen [3]. Radiation associated with CT scans may increase the possible risk of cancer, and there is no threshold dose for stochastic effects. Generally, the radiation dose from diagnostic X-ray imaging tests is considered modest, and whether there is enough data to demonstrate a cancer risk at these low levels is debated. Recent studies show that CT scans with acceptable image quality and high precision can be produced with minimal radiation exposure [2].

International standards stipulate that all CT scanners provide a radiation dose report for each examination regarding dose length product (DLP) and CT volume dose index (CTDIvol). CTDIvol offers a standard way to compare different types of CT scanners' slice-by-slice radiation levels using a reference phantom. DLP, dose length product (cm), and CTDIvol (mGy) represent the overall irradiation energy to the reference phantom. Furthermore, CTDIvol is a CT exposure index determined from a polymethyl methacrylate (PMMA) phantom, available in two sizes, 32 and 16 cm [4]. The American Association of Physicists in Medicine (AAPM) Report 204 describes the method by which scanners display dose metrics; the volume-weighted computed tomography dose index (CTDIvol) can be adjusted to include individual patient sizes and is referred to as a size-specific dose estimate (SSDE) [5]. Another method is based on measurements using thermoluminescence dosemeters (TLDs) implanted at various organ positions in an anthropomorphic phantom [6, 7]. Although TLD dosimetry is considered the standard method for measuring

the absorbed dose in a phantom, its dose measurement is laborious and time-consuming.

It is crucial to evaluate the dose and image quality between different protocols for patients of all sizes to ensure patient-specific examinations with reduced radiation doses but acceptable image quality. This is especially important considering the high prevalence of obesity in the screened population and the repeated radiation exposure during screening programs [8]. Currently, there is no official national or international protocol specifically regulating low-dose pediatric CT examinations. Some studies have only reduced tube voltage and current below standard levels to achieve low-dose imaging. Therefore, to achieve a low dose while maintaining good image quality, this research adapted the AAPM pediatric routine chest protocol as the standard-dose pediatric examination protocol. This adaptation involved decreasing both the tube voltage and current in the AAPM protocol until the CTDIvol value reached half of the standard examination's CTDIvol.

This study examined pediatric phantoms of various sizes aged 7 years, an in-house pediatric phantom representing a 7-year-old is utilized due to the complete development of internal organs at this age, while still being representative of a child. Using both low-dose tube voltage and standard doses to achieve precise and detailed imagery with the lowest possible dose. Comparison of SSDEs and diameter effectiveness of pediatric in-house phantoms used by low-dose and standard-dose techniques were investigated. In addition, the performed image quality to produce an acceptable CT dose index and diagnostic image quality for in-house pediatric phantoms was investigated using targets as healthy tissue in the lung organs with the AAPM 204 protocol.

II. METHODOLGY

The in-house phantom pediatric design created used pediatric Thorax DICOM data for CT obtained from The Cancer Imaging Archive (TCIA) [9] and the document of the registered patent by Endarko *et al.* [10]. The data taken is 7 years. Fig. 1 illustrates the fabricated in-house pediatric phantom for 7 years old and how unhealthy targets present tissue; it used 12 artificial pulmonary targets in four diameter sizes (3, 5, 8, and 10 mm) sorted from smallest to largest diameter and CT densities (+100, -400, and -750 HU). The artificial targets were made with Polylactic Acid (PLA).

Chest CT protocol in pediatrics following the AAPM Pediatric Routine Chest CT Protocol reference [1]. Our study uses low-dose and standard-dose CT scanners GE Revolution Evo 128 Slice (Table I). This study's helical mode caused the images to continuously shorten scanning time, lower radiation exposure, and improve diagnostic accuracy.

LD-V1 film calibration is carried out after calibration for the reference dosimeter, namely the Raysafe X2 ion chamber. After that, calibration was carried out for LD-V1 film by irradiating the film using a CT-Scan 128 Slice aircraft. The film is taken as one part of one batch sheet, then cut into pieces of 3 × 3 cm. The first step in the film irradiation process is placing the film in a precise position with the radiation source. Scans were then carried out on the parameters of 80 kV voltage, 50-300 mAs tube current, and the same position as the laying of the Raysafe X2 ion chamber. After that, the irradiated LD-V1 film is then scanned using a scanner (Epson Perfection V850 Pro). The format settings used in scanning are 720 dpi resolution, 48 bits, and saved in TIFF format. The software used to analyze scanner results from film is ImageJ software. The region of interest (ROI) measured 1010 mm for each Gafchromic LD-V1 film. Gafchromic LD-V1 film background correction using analysis method. The net pixel value (net PV) can then be calculated using the formula below by subtracting the average pixel value before and after irradiation [2].

$$netPV = |PV_{after} - PV_{before}| \tag{1}$$

where PV_{after} and PV_{before} is the average value of a pixel value. The results obtained will be in the form of pixel values. Pixel data is obtained in 3 channels: red, green, and blue. The pixel results on the three channels will later be plotted in a calibration curve of radiation changes in reflectance calculated using pixel value (PV) obtained from ROI results [3].

Dosimetry was evaluated to determine the use of low doses received by in-house pediatrics phantom with various sizes. CTDIvol is a dose index that provides information about the scanner output for a standard condition [4], [5]. However, the dose received by the patient depends on both patient size and scanner output. AAPM Report 204 introduced a new metric, the SSDE, which can be used to estimate average patient dose based on the CTDIvol and linear patient size measurements. To evaluate the dose on CT scan according to AAPM Task 204 based on measurements on the patient's diameter, SSDE is calculated from the CTDIvol value found in equation (6). However, the CTDIvol value is obtained on the CT-Scan console on the screen using tabulation adjustment variables based on effective diameter to estimate the number of doses in each patient [6, 7].

$$CTDI_w = \frac{1}{3}CTDI_{100}^{center} + \frac{2}{3}CTDI_{100}^{periphery} \tag{2}$$

$$CTDI_{vol} = \frac{CTDI_w}{pitch} \tag{3}$$

$$SSDE = f_{size}^{32} \times CTDI_{vol}^{32} \tag{4}$$

where CTDI_w is the weighted average dose across a single slice and pitch is the distance of the table moving in one 360° gantry rotation. f_{size}^{32} size is a conversion factor based on the effective diameter and CTDI_{vol} specified in the AAPM 204 report on SSDE. The CTDI_{vol} is the average absorbed dose inside a scan volume concerning a standard 32 cm CT phantom diameter. The conversion factor values were derived from the DICOM header [6]. CTDI_{100} can be measured at the center of the phantom and the periphery, resulting in $CTDI_{100}^{center}$ for the center and $CTDI_{100}^{periphery}$ for the peripheral measurement. It is emphasized that the quantity measured for CTDI_{100} defined in this document is air kerma [8].

Towards the left lung are targets with diameters of 10 and 8 mm, and in the right lung, there are targets of 5 and 3 mm in diameter with different densities (+100, -400, and -750 HU)

TABLE I: Protocol chest CT-Scan Pediatric.

Parameter	Low kV-increase tube current			Standard kV-increase tube current		
	L1	L2	L3	S1	S2	S3
Tube voltage (kV)	80	80	80	120	120	120
Tube current (mA)	50	70	100	50	70	100
Reconstruction	FBP	FBP	FBP	FBP	FBP	FBP
Rotation time (s)	0.5	0.5	0.5	0.5	0.5	0.5
Slice thickness (mm)	3	3	3	3	3	3
FOV (mm)	250	250	250	250	250	250
Acquisition mode	Helical	Helical	Helical	Helical	Helical	Helical
Pitch	1	1	1	1	1	1
Matrix	512 x 512	512 x 512	512 x 512	512 x 512	512 x 512	512 x 512
Collimation	16 x 1.5	16 x 1.5	16 x 1.5	16 x 1.5	16 x 1.5	16 x 1.5

Protocol L1-L3: Low dose.
Protocol S1-S3: Standard dose.

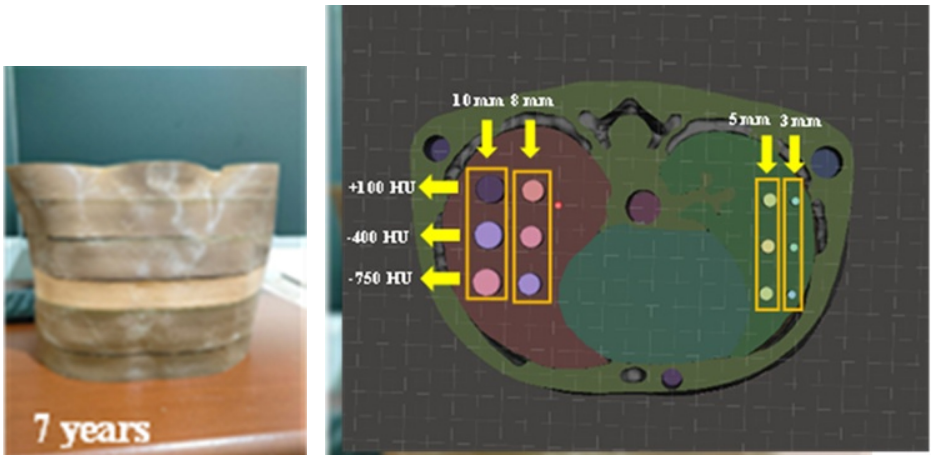

(a) (b)

FIG. 1: The fabricated in-house phantom: a) the pediatric phantom for 7-year-old, and b) targets present unhealthy tissue with diameter sizes of 3, 5, 8, and 10 mm sorted from smallest to largest diameter..

(Fig. 1). A region of interest (ROI) measuring 4 $\times$ 20 pixels (Fig. 2) was carried out on the variation in targets diameter using ImageJ software to obtain the pixel mean result. Image quality analysis is carried out to determine whether the results of the image produced are good or not. The study focused on using low doses but good image quality with the first experiment, an in-house pediatric phantom variation of various sizes that would be compared using CT-Scan GE Revolution Evo 128 Slice. The second experiment was on variations in low tube voltage CT-Scan, low tube current (50 mAs), and standard dose (100 mAs); there were four different targets diameters of 3, 5, 8, 10 mm, and CT densities of each diameter of +100, -400, -750 HU contained in the lungs in a slice in-house pediatric phantom.

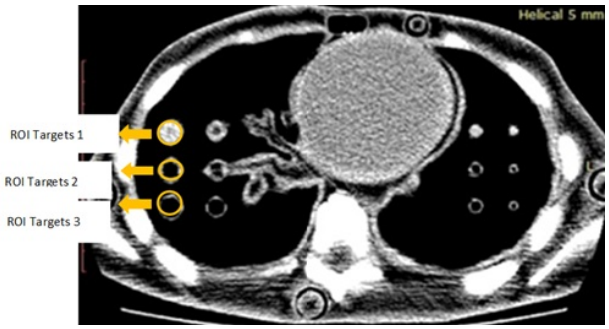

FIG. 2: In house pediatric phantoms 7 years with 3 various targets and densities +100, -400, and -750 HU, respectively.

Image quality analysis using SNR and CNR, Signal to Noise Ratio is a parameter in image quality to compare between signal and noise. Image signals are directly related to the number of photons detected, whereas noise can be seen as stochastic fluctuations of pixels in the area around their average value. SNR analysis can be calculated using eq. (5).

$$SNR = \left\| \frac{HU_{ROI}}{\sigma_{ROI}} \right\| \tag{5}$$

where HU_{ROI} is the average value of HU that the object receives in the ROI. σ corresponds to the standard deviation of

image noise in the ROI [9].

The contrast of the image depends on the energy of the photons. Image noise depends on the number of photons used to create the image. However, noise is inherently irrelevant if the contrast level is high, whereas noise becomes especially important if the intrinsic contrast is low. In practice, the contrast-to-noise ratio (CNR) is a key determinant of CT image quality. If the CNR level is high, detection of lesions will be easy. Low CNR will limit lesion detection and can be improved either by increasing contrast or by reducing noise [10].

$$CNR = \frac{|HU_{ROI} - HU_{Axillary-fat}|}{\sqrt{\frac{\sigma^2_{ROI}+\sigma^2_{Axillary-fat}}{2}}} \quad (6)$$

where the formula above as the standard deviation of image noise in ROI. In the CNR formula is obtained considering the fat on the body as a reference [9]. The following is a flowchart illustrating the research process (Fig. 3).

III. RESULT AND DISCUSSION

A. LD-V1 Film Calibration

Calculating the value of net R, such as equation (1) contained in the radiochromic film protocol called the calibration curve, is necessary to assess the response of LD-V1 films in each channel. Pixel values are obtained from measurements using ImageJ software by creating an ROI of 1010 mm on scanned film. Furthermore, the dose-response curve using polynomial fittings can be seen in Fig. 3. Polynomial equations are obtained on red, green, and blue channels. Using polynomial fittings based on Devic's research reference, 2016 because LD-V1 film in CT-scan modality is the best method by showing the lowest uncertainty and error values [11].

GafChromic LD-V1 film has a four-layer laminate configuration consisting of outer layers of orange and white polyester substrates (97 m) and a pressure-sensitive adhesive (20 m) connecting the orange substrate to the active layer (20 m). According to the manufacturer specifications, LD-V1 is designed for measurement in the nominal X-ray energy range of 40 kV to 160 kV and dose range of 20 mGy to 200 mGy (Ashland Inc, Wilmington, DE, USA). In contrast, the older XR-QA2 was specified for an X-ray energy range of 20 kV to 200 kV and a dose between 1 and 200 mGy.

Fig. 3 shows the film's response to the dose, expressed in the value of the change in reflectance (net R). The calculation is used by the reflectance method because the LD-V1 film is a reflection-type film. It was found that the red channel had better sensitivity than the green and blue channels because the curves on the red channel showed a larger band of variation in the green and blue channels. In research conducted by Casolaro, it is stated that the LD-V1 Gafchromic film has a maximum sensitivity wavelength range between 600 - 645 nm; this can also be the basis for why the sensitivity is best in the red channel because the wavelength range of LD-V1 Gafchromic film is close to the red wavelength range of 620-750 nm [12].

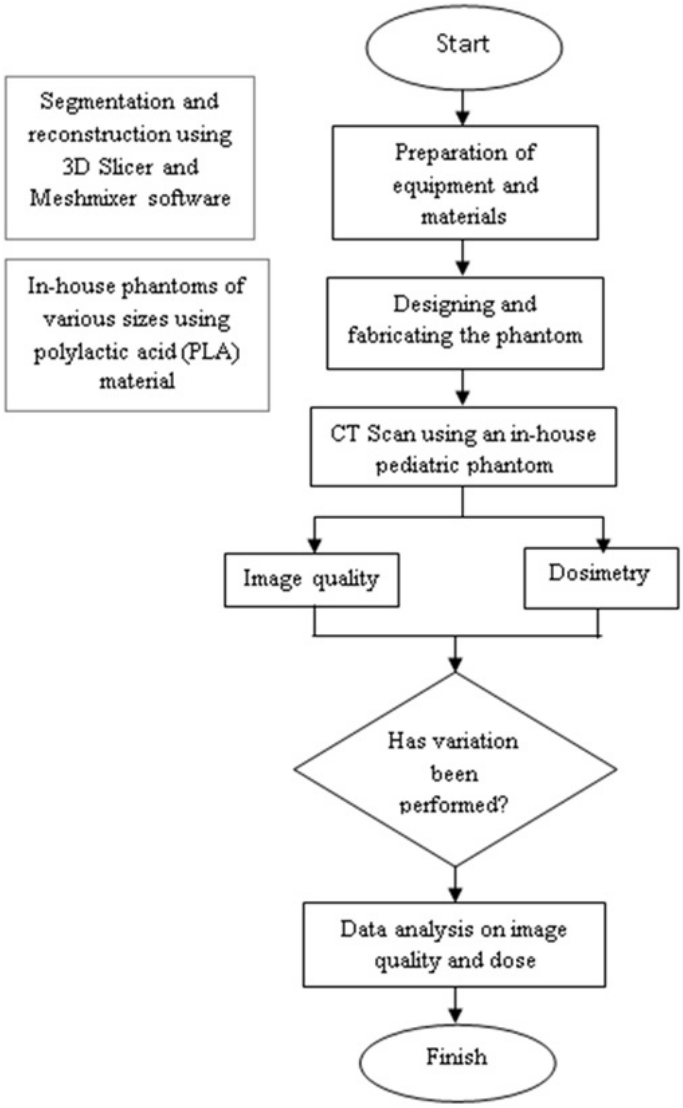

FIG. 3: Flowchart in the research.

The polynomial fitting equation of order 3, according to [11] polynomial fittings in the CT modality, is the best method because it shows the lowest uncertainty and error values. Here is the equation of the polynomial obtained and the R-squared that approximates the conformity (Table II).

B. Dosimetry Evaluation

The calculation results of CTDIvol by consol, CTDIvol (mGy), and SSDE were obtained by measuring low and standard tube currents (50, 70, and 100 mAs) using variations in current voltages with in-house pediatric phantom of various sizes.

Table III shows the dosimeter evaluation on an in-house pediatric phantom with effective diameter values obtained from AP+LAT and following AAPM 204 protocol on pediatric thoracic size. Thus, conversion coefficients obtained in this

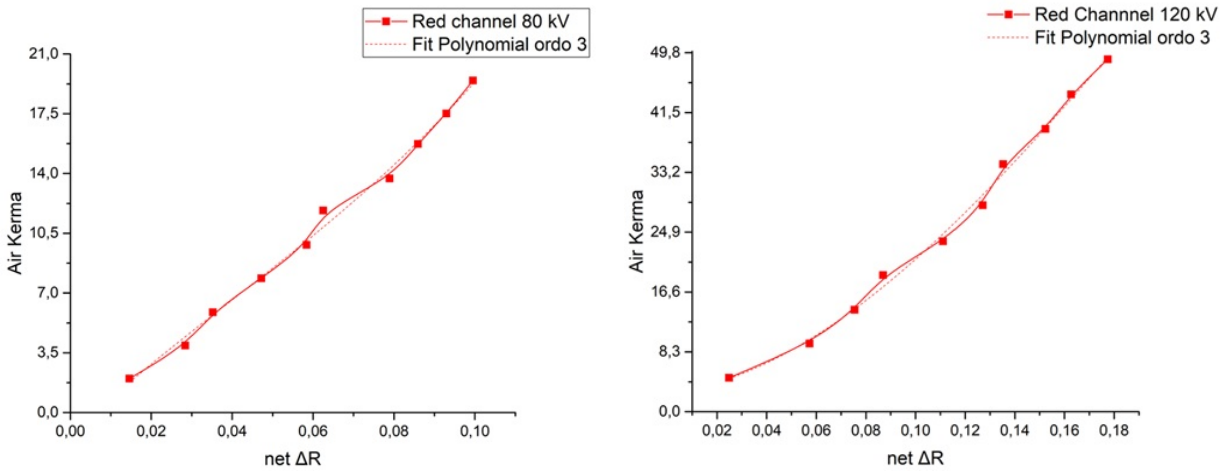

(a) (b)

FIG. 4: Calibration graph at voltages (a) 80 and (b) 120kV with CT-Scan 128 Slices.

TABLE II: Polynomial fittings calibration equation at tube voltages of 80 and 120 kV.

Channel	Polynomial Equation	R-Square
Red tube voltage 80 kV	$y = 7559.3x^3 - 901.23x^2 + 221.01x - 1.2812$	0.994
Red tube voltage 120kV	$y = -2708.3x^3 + 1753x^2 + 36.664x + 2.6689$	0.995

TABLE III: A comparison of CTDI vol and SSDE value with different patients effective diameter.

Age	CT protocol	CTDIvol (mGy)	SSDE (mGy)
7 years	L1	0.70	3.71
	L2	0.99	3.95
	L3	1.41	4.10
	S1	2.10	6.09
	S2	2.94	6.52
	S3	4.21	10.86

study can be used with CTDIvol calculated based on 32 cm body phantom. Some abdominal examinations of children are based on 16 cm head phantom [13]. The effective value of the diameter for 7 year old was 20.15 cm. Based on the results of CTDIvol above, every increase in tube voltage, the greater the CTDIvol value, this is influenced by the voltage difference between the anode and cathode, the electrons that move faster and X-rays will have a higher average energy and the radiation dose will be higher as well [14]. Similarly, with a voltage of 120 kV, receiving a greater absorbed radiation dose as indicated by the polynomial decreasing SSDE value as the size of the pediatric in-house phantom increases. Another study assessing SSDE in CT reported that patient size affected CTDIvol but not on SSDE, concluding that increasing the scanner output for larger patients would not necessarily increase the mean absorbed dose to the patient [15].

C. Image Quality Analysis

SNR calculation results were obtained at 7 years with tube and current-voltage variations. For image quality analysis, targets with densities +100 HU, with four diameters targets of 3, 5, 8, and 10 mm, respectively, are in both lungs. Below is the SNR result curve with the influence of voltages of 80 and 120 kV on the diameter targets variation (Fig. 4).

Fig. 6 shows the effect of diameter targets on voltages of 80 and 120 kV with phantom variations of various sizes at densities of +100 HU. SNR image quality evaluations are classified based on target diameters (3, 5, 8, and 10 mm), and skin. A large SNR value indicates that the object can be clearly distinguished from the background, therefore the image of the object is not obscured by the background. Fig. 6 provides information that the SNR value is lowest at a voltage of 120 kV and the lowest at a voltage of 80 kV. This proves that when the voltage rises, the acceleration of electrons is faster, and the greater the energy, the greater the penetrating power passing through the network. So that voltage affects the quality of the image produced and affects the SNR value [16]. Thus, it can be said that the increase in voltage will be proportional to the increase in SNR value.

Fig. 5(a) shows a pediatric in-house phantom at the age of 7 years with helical scanning obtained at a tube voltage of 80 kV having higher noise than at a voltage of 120 kV (Fig. 6(b)). It can be explained that a decrease in kV or mAs will cause a decrease in the noise level of the image and reduce the ability to detect low contrast. However, noise should not be an important factor because the organs studied inherently

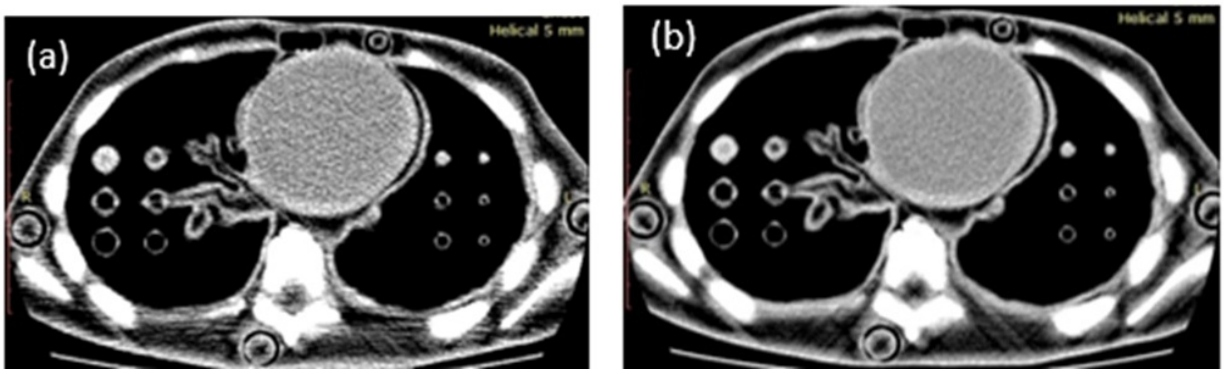

(a) (b)

FIG. 5: Helical image of a 7-year-old pediatric in-house phantom with (a) using a tube voltage of 80 kV and (b) using a tube voltage of 120 kV.

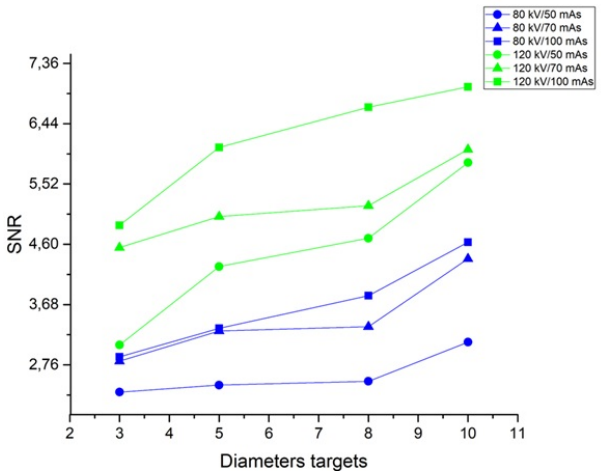

FIG. 6: The effect of the diameter targets on image quality with voltages of 80 and 120 kV with in house pediatric phantom (7 years).

show high contrast in bone and soft tissues [17].

The limitation of our study is that targets are made using only one type of material, and targets are made only calculated diameter and level of HU. Therefore, for future studies, the material for targets can be varied to obtain a good value image quality. Moreover, the manufacture of targets can be added in terms of volume to calculate the volume of the targets.

IV. CONCLUSION

In the current study, in-house pediatric phantoms were successfully created to analyze dose and image quality in radiodiagnostics. For image quality use, the low-dose CT protocol has a detection sensitivity of 100% for targets measuring ¿ 5mm in diameter. SSDE considers patient size and provides a more accurate reflection of patient dose than CTDIvol. When considering SSDEs for patients of different body sizes, a protocol that balances diagnostic reception with dose reduction should be undertaken. Further research focused on targets diameter and type to be further investigated for the calculation of image quality of in-house pediatric phantom of various sizes.

Acknowledgments

The authors are thankful to the management of the Dharmais Cancer Hospital Jakarta for the permission to conduct the study and collect and analyze data at the Radiodiagnostic Facility. This study was funded by the Institut Teknologi Sepuluh Nopember (ITS) and Kemendikbudristek under Penelitian Dasar Unggulan Perguruan Tinggi (PDUPT) (No. 1988/PKS/ITS/2023).

[1] M. Rawashdeh, *et al.*, "A new approach to dose reference levels in pediatric CT: Age and size-specific dose estimation," Radiat. Phys. Chem., vol. 205, Apr. 2023, doi: 10.1016/j.radphyschem.2022.110698.

[2] N. Hustings, H. Bosmans, and S. Dymarkowski, "Pursuing Optimal Radiation Dose in Pediatric Cardiac CT: A Report from University Hospital Lueven, Radiat. Prot. Dosimetry, vol. 198, no. 3, pp. 139-146, Mar. 2022, doi: 10.1093/RPD/NCAC007.

[3] A. Almujally, *et al.*, Evaluation of paediatric computed tomography imaging for brain, and abdomen procedures, Radiat. Phys. Chem., vol. 200, Nov. 2022, doi: 10.1016/J.RadpPhyChem.2022.110271.

[4] J.A.S. Jerrold,*et al.*, The Essential Physics of Medical Imaging, Third Edition., Med. Phys., vol. 40, no. 7, p. 077301, Jul. 2013, doi: 10.1118/1.4811156.

[5] M. Kiani and A. Chaparian, "Evaluation of image quality,

organ doses, effective dose, and cancer risk from pediatric brain CT scans," Eur. J. Radiol., vol. 158, Jan. 2023, doi: 10.1016/J.EJRAD.2022.110657.

[6] J. Boone, *et al.*, AAPM report No. 204: Specific Dose Estimates (SSDE) in Pediatric and Adult Body CT Examinations," 2011. Accessed: Apr. 02, 2023. [Online]. Available: https://www.aapm.org/pubs/reports/detail.asp?docid=143

[7] M.M. Mille, *et al.*, Fabrication of a pediatric torso phantom with multiple tissues represented using a dual nozzle thermoplastic 3D printer," J. Appl. Clin. Med. Phys., vol. 21, no. 11, pp. 226-236, Nov. 2020, doi: 10.1002/ACM2.13064.

[8] I. Barreto, *et al.*, Patient size matters: Effect of tube current modulation on size-specific dose estimates (SSDE) and image quality in low-dose lung cancer screening CT," J. Appl. Clin. Med. Phys., vol. 21, no. 4, pp. 87-94, 2020, doi: 10.1002/acm2.12857.

[9] P. Jorda, *et al.*, Pediatric chest-abdomen-pelvis and abdomen-pelvis CT images with expert organ contours," Med. Phys., vol. 49, no. 5, pp. 3523-3528, May 2022, doi: 10.1002/mp.15485.

[10] Endarko, and A. P. Hariyanto, "Teknik mendesain dan fabrikasi fantom antropomorfik toraks pasca masektomi", Indonesia Patent. 2022; P00202102195.

[11] F.D.-A.C. dose Summit, "Pediatric Routine Chest CT Protocol, Accesed Mei 20, 2025. https://www.aaapm.org/pubs/CTProtocols/.

[12] X. Zhu, J. Yu, and Z. Huang, "Low-dose chest CT: Optimizing radiation protection for patients," Am. J. Roentgenol., vol. 183, no. 3, pp. 809-816, 2004, doi: 10.2214/ajr.183.3.1830809.

[13] E. Nakajima, and H. Sato, "Characterization of a new radiochromic film (LD-V1) using mammographic beam qualities," Z. Med. Phys., Jun. 2023, doi: 10.1016/j.zemedi.2023.05.004.

[14] N. Tomic, *et al.*, "Characterization of calibration curves and energy dependence GafChromicTM XR-QA2 model based radiochromic film dosimetry system," Med. Phys., vol. 41, no. 6, 2014, doi: 10.1118/1.4876295.

[15] R. L. Dixon, "A new look at CT dose measurement: Beyond CTDI," Med. Phys., vol. 30, no. 6, pp. 1272-1280, Jun. 2003, doi: 10.1118/1.1576952.

[16] R. Aryawijayanti, "Analitisi Dampak Radiasi Sinar-X pada Mencit Melalui Pemetaan Dosis Radiasi di Laboratorium Fisika Medik," Universitas Negri Semarang, 2015.

[17] X. Xie, *et al.*, "Sensitivity and accuracy of volumetry of pulmonary nodules on low-dose 16- and 64-row multi-detector CT: An anthropomorphic phantom study," Eur. Radiol., vol. 23, no. 1, pp. 139-147, Jan. 2013, doi: 10.1007/s00330-012-2570-7.